

# Estimation of Above-ground Biomass in Mt. Apo Natural Park in the Southern Philippines Using Terrestrial LiDAR System

Ligaya C. Rubas-Leal ✉ • Robert A. Washington-Allen • Sorin C. Popescu • J. Richard Conner

Texas A&M University, UNITED STATES

## Abstract

Extraction of plot-level field measurements entails a rigid and time-consuming task. Fine resolution remote sensing technology offers an objective and consistent method for estimation of forest vertical structures. We explored the development of algorithms for estimating above-ground biomass (AGB) at the plot level using terrestrial LiDAR system (TLS). This research follows IPCC Tier 2 approach, by combining field and remote sensing data, in estimating forest carbon stocks. Permanent plots (30 × 30 m diameter) were established inside Mt. Apo Natural Park. Forest inventory was conducted in July 2013, recording tree heights and stem diameters for all hardwood species with diameter at breast height (DBH) ≥ 5 cm in three management zones: multiple use, strict protection, and restoration. Quadratic mean stem diameter was employed for large DBH intervals for deriving midpoint biomass. Three tropical allometric equations were used to derive referenced biomass values. Regressions results showed satisfactory modeling fit in relating plot-level AGB to DBH class size: 80%–89%. Mean tree heights from field and TLS data were related showing  $R^2 = 88\%$ . TLS variables derived include percentile heights and normalized height bins at 5-m intervals. The generalized linear model is a more robust model for percentile heights, while stepwise regression showed a better regression performance for normalized height bins. Strict protection zone contained the highest carbon storage. This study demonstrated the significant TLS-derived metrics to assess plot-level biomass. TLS scanning is also the first work to be done in this ASEAN Natural Heritage Park, which is constrained with local insurgency problems. Biomass in plot-level can be used to extrapolate to landscape-level using available multispectral or radar imagery.

**Keywords:** above-ground biomass • height bins • Mt. Apo Natural Park • terrestrial LiDAR system

**Correspondence:** LC Rubas-Leal. Department of Ecosystem Science and Management, Texas A&M University, United States. Email: ligayarubas@yahoo.com

**Author Contribution:** LRL conceptualized the study, conducted and led the data collection, analyzed and interpreted the data, and prepared the draft of the manuscript; RWA assisted in the data collection; SCP provided guidance during the data analysis; JRC provided funds for fieldwork and assisted in the coordination with the research site; and RWA, SCP, and JRC assisted in critically revising the manuscript.

**Editor:** Eufemio T. Rasco, Academician, National Academy of Science and Technology, PHILIPPINES

**Received:** 26 March 2016

**Accepted:** 15 December 2017

**Published:** 29 December 2017

**Copyright:** © 2017 Rubas-Leal et al. This is a peer-reviewed, open-access journal article.

**Funding Source:** Research funding by Texas A&M AgriLife Research. Fieldwork expenses covered by Texas A&M University internal funding sources: 2013 Harry Wayne Springfield Research Award and 2013 Office of Graduate and Professional Studies Research Grant.

**Competing Interest:** The authors have declared no competing interest.

**Citation:** Rubas-Leal LC, Washington-Allen RA, Popescu SC, Conner JR. 2017. Estimation of above-ground biomass in Mt. Apo Natural Park in the Southern Philippines using terrestrial LiDAR system. Banwa B. 12:res005.

# Estimation of Above-ground Biomass in Mt. Apo Natural Park in the Southern Philippines Using Terrestrial LiDAR System

**Ligaya C. Rubas-Leal** ✉ •

**Robert A. Washington-Allen** •

**Sorin C. Popescu • J. Richard Conner**

Texas A&M University, UNITED STATES

## Introduction

Measurement and quantification of forest structure is a vital step in developing a better understanding of how forest ecosystems work (Drake et al. 2002). The ability to estimate forest biomass is an important step in estimating the amount of carbon in terrestrial vegetation pools and relating its significance to global carbon cycle studies. The terrestrial LiDAR system (TLS) offers the benefit of extracting forest structural metrics at the plot level, which are cost-effective compared to rigid field measurements. These vertical structures can be used to estimate above-ground carbon storage (Lefsky 2010). LiDAR remote sensing provides the technological capability to assess woody plant structures at a high level of detail, thereby allowing more accurate estimates of biomass over large geographic areas.

TLS technology provides objective and consistent, though not necessarily unbiased, measurements due to the influence of scanner parameters, scan resolution, speed, and pulse duration (Pueschel 2013). To increase accuracy in the extraction of tree metrics, objects should be scanned from multiple locations to reduce shadowing or occlusion of background objects by foreground objects. Basic inventory tree metrics that have shown accuracy in extraction are the following: tree location, stem density, and diameter-at-breast-height (DBH). Other important metrics, however, such as tree height and stem volume have not so far been retrieved with high accuracy.

In the Philippines, various studies have been conducted in selected forest sites aimed at estimating carbon storage. First, Han et al. (2010) piloted a study using a destructive sampling approach from 2007 to 2008 at Mt. Makiling Forest Reserve. Their study aimed to compare the carbon storage and flux between a sixty-year-old secondary natural forest stand and a large-leafed mahogany plantation. Their results showed that the total carbon storage in above-ground biomass, litter layer, and soil of the secondary forest stand was 313.12 Mg C ha<sup>-1</sup>, which is 1.7 times larger than the carbon storage of the large-leafed mahogany plantation, estimated at 185.28 Mg C ha<sup>-1</sup>. Second, Lasco et al. (2004) also conducted a non-destructive sampling of a similar study site from 1992 to 1996. They reported that secondary forest can store 418 Mg C ha<sup>-1</sup>. Finally, in the southern part of the country, Lasco et al. (2006) studied the effects of selective logging on carbon stocks of dipterocarp forests on fixed plots using a chronosequence of one to twenty-one years after logging. They found that unlogged forests had average carbon stocks of 258 Mg C ha<sup>-1</sup>, of which 34% was in soil organic carbon (SOC). After logging, the above-ground carbon stocks declined by 50%, while changes in SOC showed no apparent relationship with number of years after logging.

Our study displays the application of Tier 2 approach as required by the Intergovernmental Panel on Climate Change (IPCC). A high-resolution TLS data was added to the field measurements in developing an algorithm for the plot-level biomass. To comply with the Reducing Emissions from Deforestation and Degradation (REDD) guidelines, the carbon content was assessed by forest type (Olander et al. 2008).

Our research attempts to provide answers to these questions: (1) How can TLS technology be helpful in developing a plot-level biomass model? (2) How does the use of referenced biomass from three tropical allometric equations perform in estimating plot-level biomass? Destructive sampling was not permitted inside the protected area, thus biomass was estimated using the referenced biomass from three allometric equations relating tree height, diameter-at-breast height, and wood specificity volume.

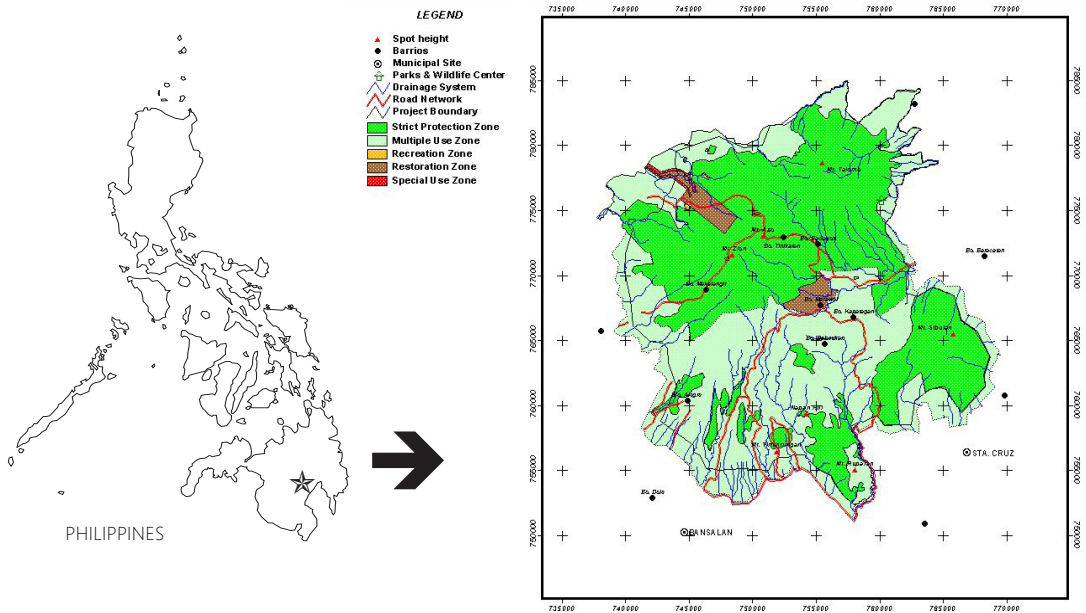


**FIGURE 1** Location of the Mount Apo Natural Park research site in Mindanao Island, Southern Philippines (Management Zone Map, right, from [www.mafi.org.ph](http://www.mafi.org.ph))

The primary objective of this study is to develop algorithms to determine above-ground biomass (AGB) at the plot level from terrestrial LiDAR data. Our specific objectives include the following: (1) relate referenced AGB values from three allometric equations to TLS variables; (2) identify meaningful TLS variables in estimating plot-level AGB; (3) demonstrate the effect of multiple scan locations on the accuracy of extracting individual tree metrics like height and stem diameter; and (4) characterize carbon content by management zone and land cover type.

## Data and Methods

### Study Site

The Mt. Apo Natural Park (MANP) is located in Southern Philippines, with primary conservation area that covers 54,974.87 ha (Figure 1). MANP is bounded by two governmental administrative regions: Region XI, which lies on the north and south portions of the park, and Region XII, which borders the western side. Its mean monthly temperature ranges from a low of 26.4 °C during January to 27.9 °C during

April. MANP elevations range from 600 m to 2954 m asl.

MANP was declared as a national park on 9 May 1936 by President Manuel L. Quezon by virtue of Presidential Proclamation No. 59. Large areas inside the park were destroyed due to human settlements and agricultural activities (Lewis 1988). In 1984, the International Union for Conservation of Nature (IUCN) declared Mt. Apo as one of the world's most threatened protected natural areas, drawing international attention. The Mount Apo Protected Area Act of 2003, or Republic Act 9237, was legislated in 2004. Mt. Apo is listed as a natural park and was established in 2007 as a World Heritage Site ([www.mafi.org.ph](http://www.mafi.org.ph)). On 18 December 2003, the Association of Southeast Asian Nations (ASEAN) declared Mt. Apo National Park as one of only two ASEAN Natural Heritage Parks in the country ([www.protectedplanet.net](http://www.protectedplanet.net)).

### Data Acquisition

Prior to conducting any fieldwork, we secured a research permit from the Mt. Apo Protected Area Management Board (PAMB).

Sixteen circular plots at 30 × 30 m diameter were scanned during the fieldwork in July 2013.

These plots were stratified across the management zones, covering the vegetation gradient in MANP. The presence of local insurgency activity prevented us from sampling additional plots. FARO Laser Scanner Focus 3D was placed in five different scan locations per plot: center, north, east, west, and south. Four scanning targets made of volleyballs mounted on 2-m-long polyvinyl chloride (PVC) pipes were positioned at each of the four sides. The scanner was mounted on a tripod at an average height of 1.48 m above ground. Each scan runs for six to nine minutes. FARO Laser Scanner Focus 3D was used with its high-speed 3D laser scanner for detailed measurement. FARO Scanner 120 is a touch-operated screen that produces images of complex environments in only a few minutes. This scanner emits a laser beam from a rotating mirror out towards the scanned area. It then distributes the laser beam at a vertical range of 305° and a horizontal range of 360°. This laser beam is then reflected back to the scanner by objects in its path. The laser emits pulses of 905 nm at 1 cm posting and 120-m range. Its multisensory capability enables it to level each scan with an accuracy of 0.015° and a range of ±5°. The scanner can detect the heights relative to a fixed point via an electronic barometer and adds it to the scan. Its electronic compass gives the scan an orientation.

A geographic positioning system (GPS Garmin III plus) was used at the center tree to record the plot location. A laser hypsometer provided measurements of horizontal distance, tree height, and azimuth. A spherical densiometer was used to measure canopy cover and its complement, the gap fraction. A Kestrel weather unit was also employed to provide information on elevation, temperature, and relative humidity. A prism was used to estimate forest basal area. Finally, a compass was used initially to locate directions to guide where to place the scan targets.

All hardwood trees with at least 5-cm diameter within the circular plot were tagged using a standard stick of 1.34 m. Individual species for hardwood trees were identified by local names with the help of a native guide. Diameter-at-breast-height (DBH), height, and canopy width were measured for all trees with

DBH > 5 cm. Canopy cover and basal area index were also recorded for the plot.

## Data Analysis

*Scan preprocessing and registration.* Directional raw FARO laser scans were registered using FARO SCENE software. Preprocessing was applied to detect spheres used as scanning targets. Scans were registered with the use of at least three reference objects per scanned image. Correspondence view was generated and registration results with weighted statistics were shown. An option was chosen to level scans according to inclinometer. The value tension describes the discrepancy in the global coordinate system between the position and orientation of the two corresponding reference objects in at least two scans. Values close to zero indicate a good registration result.

Registered scans were exported as point cloud and saved as XYZ format. These ASCII data were then transformed into \*.txt file format using SURFER software. SURFER is a full-function 3D visualization, contouring, and surface modeling program. Its interpolation engine transforms ASCII data into more useful 3D surface mapping.

*Vegetation height metrics.* The transformed ASCII files were imported into the Quick Terrain Modeler ([www.appliedimagery.com](http://www.appliedimagery.com)). QTM is a three-dimensional point cloud terrain visualization software package designed for processing LiDAR data. Above-ground-level (AGL) analysis was applied with grid sampling of 1 m and registered using a global coordinate system of Universal Traverse Mercator (UTM) with zone of 51N. AGL analysis is a powerful tool within the QTM software that enables it to convert the absolute elevations into relative heights. This tool removes ground and facilitates extraction of vertical heights to every point cloud. A circular plot was extracted using LASTools software to show a 15-m plot boundary. This process begins with an acquisition of the coordinates for the center tree. The point clouds from the circular plot were clipped below an elevation of 2 m.

The resulting image provides the plot vegetation with height above 2 m. This vegetation

height model was then processed in FUSION software to extract percentile heights and normalized bin heights. FUSION software enables command line programs designed specifically for LiDAR data processing.

There were two sets of height metrics generated from the model. The first set consists of point cloud statistics related to mean height, maximum height, height standard deviation, and percentile heights. The second set of height metrics is the normalized height metrics. Height bins were classified as 2 to 5 m, 5 to 10 m, up to 40 to 45 m. Normalized height bin (NHBin) metrics are derived using Equation 1:

$$NHBin(i) = \frac{\text{Returned points for bin (i)}}{\text{Sum of all total returned points}} \quad \text{for } i = 5, 10, \dots, 45 \quad (1)$$

Regression modeling was employed to relate the above-ground biomass derived using three tropical allometric equations to the height statistics. Two types of regression models were chosen to evaluate the goodness of fit. Generalized linear model (GLM) using maximum likelihood estimation was considered to assess the relationship between these predictor variables. This method estimates the parameters of a statistical model, with the assumption that tree heights are normally (Gaussian) distributed with some unknown mean and variance. The

second regression model used is stepwise regression. A forward selection was chosen that automatically adds variables that improve the model fit. A variance inflation factor (VIF) was also derived for the significant parameters in the stepwise regression to detect the presence of multicollinearity in the data.

*Height and DBH stem maps.* Height and DBH stem maps were plotted on a Cartesian plane for each plot. The reference tree is the center tree with (0,0) coordinates. Trees within the plot are mapped using the azimuth and horizontal distance information (Figure 2).

These stem maps provide an aerial display of the location for each tree within a plot with reference to the center tree. In the first step of the mapping process, an adjusted angle was computed, which is the difference between 360° and angle (Ø) for a specific tree. Then polar coordinates were computed using the adjusted angle and its relation to the angle size of a tree, multiplied with a constant factor to convert degrees to radians.

$$\text{Adjusted angle} = 360^\circ - \varnothing \quad (2)$$

$$\text{Polar coordinates} = (\text{Adjusted angle} + 270^\circ) \times 0.0174532925 \quad (3)$$

$$\text{Polar coordinates} = (\text{Adjusted angle} - 90^\circ) \times 0.0174532925 \quad (4)$$

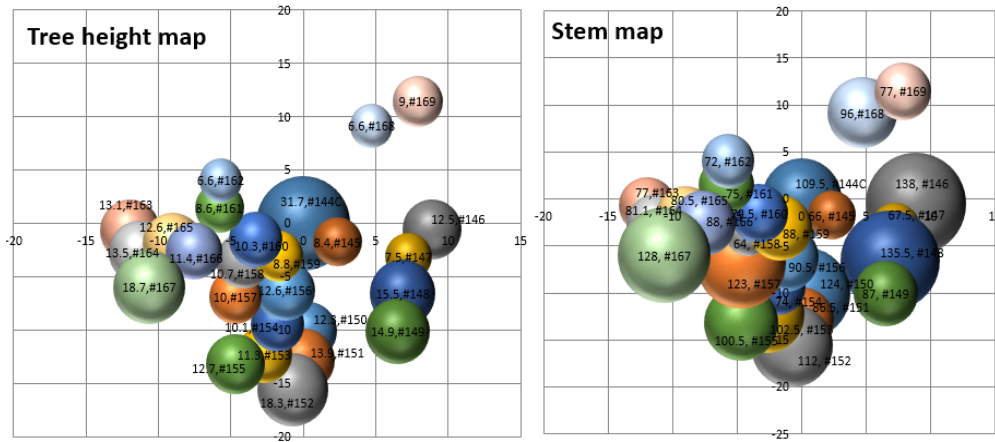


**FIGURE 2** Tree height map and stem map of a study plot inside a multiple use zone



*Field biomass generation.* Biomass density is estimated based on the biomass per average tree of each DBH class multiplied by the tree density in the class. Trees in each plot were classified based on DBH class. The DBH classes are as follows: 5 to 50 cm, 51 to 100 cm, 101 to 150 cm, 151 to 200 cm, 201 to 250 cm, 251 to 300 cm, and above 300 cm. Tree density was computed as the number of trees present per plot based on each DBH class. The midpoint of each class was computed based on the quadratic mean stem diameter (QMSD). Brown (1997) suggested the use of QMSD as a better choice, compared to the average DBH, particularly for wide diameter class. QMSD is defined as the DBH of a tree of average basal area in the class. This is derived by first computing for the basal area (BA) of the average tree. Then QMSD is derived as two times the square root of BA divided by  $\pi$  (i.e., 3.1416).

$$\text{Basal area of average tree} = \frac{\text{BA of the diameter class}}{\text{No. of trees in the DBH class}} \quad (5)$$

$$\text{Quadratic mean stem diameter} = \frac{\text{BA of the diameter class}}{\text{No. of trees in the DBH class}} \quad (6)$$

After computing the midpoint of the DBH class, tree biomass was calculated using the three tropical allometric equations. Then biomass of all trees was computed as the product of tree density and QMSD per DBH class. Total above-ground biomass per plot ( $\text{Mg plot}^{-1}$ ) was computed as the summation of all biomass of trees in all DBH class.

*Referenced biomass.* Plot-level above-ground biomass was estimated using three allometric equations developed by Brown (1997), Ketterings et al. (2001), and Chave et al. (2005), respectively.

Brown (1997) allometry is expressed as follows:

$$\text{Total above-ground biomass (TAGB)} = \exp(-2.134 + 2.53 \ln(\text{DBH})) \quad (7)$$

where TAGB is total above-ground biomass in  $\text{kg tree}^{-1}$  and DBH is in cm.

Ketterings et al. (2001) developed an equation as follows:

$$\text{Total above-ground biomass (TAGB)} = r p^{\text{avg}} (\text{DBH})^{2+c} \quad (8)$$

where  $r$  is a parameter that is constant over wide range of geographical areas,  $p^{\text{avg}}$  is the average wood density for the study area, and  $c$  is the parameter estimated by relating DBH and  $H$ . Ketterings et al. (2001) used these values:  $r$  is 0.11,  $p^{\text{avg}}$  is  $0.604 \text{ g cm}^{-3}$ , and  $c$  is 0.397.

Chave et al. (2005) generated an allometric equation as follows:

$$\text{Above-ground biomass (AGB)} = \frac{\exp(-2.977 + \ln(pD^2H))}{0.0509 \times pD^2H} \quad (9)$$

where  $p$  is the species-specific wood density ( $\text{g cm}^{-3}$ ),  $D$  is the DBH (cm), and  $H$  is height (m).

Figure 3 displays the image processing flowchart for the terrestrial laser scan data.

## Results and Discussion

Permanent plots were sampled covering 697 hardwood trees from three types of management zone: multiple use (MU), strict protection (SP), and restoration (R). Plots established per zone are: MUZ (9), SPZ (2) and RZ (5). Limited sampling plots were also discussed in Ribeiro et al. (2013) that was evenly distributed across the vegetation gradient.

Mahogany trees were mostly present in MUZ with average heights of 20 to 23 m. RZ shows a shorter height distribution, with most trees at 10 to 13 m tall. SPZ shows the presence of multi-stemmed trees found in the upper montane type. Tree heights are mostly lumped in the lower height at 6 m tall, with few taller trees.

## Scan Registration

Scan merging showed higher deviation results with a range from 0.02 to 3.16. Values close to zero signify good results. These results indicate that target scans or reference objects were not accurately detected during point-cloud registration. The four targets were not all detected at all times from the center scan. There were also instances where only one target is detected from any directional scan.

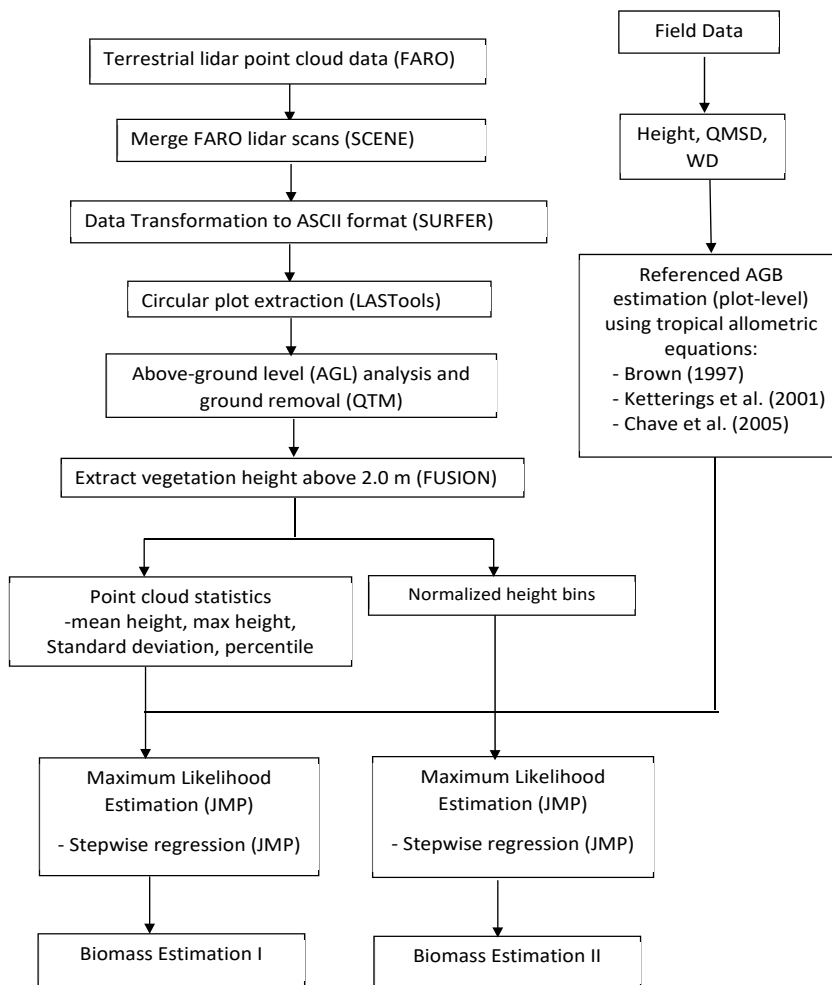


**FIGURE 3** Data processing flow chart for terrestrial laser scan data

To remedy this issue, similar-looking objects (e.g., branches, hanged backpacks) were identified between scans to allow point cloud registration. Initial attempts were made to do tree-level AGB analysis, but an inspection of these point clouds discouraged us from further work on this research objective. Therefore, we directed our efforts to doing plot-level AGB estimation.

Height metrics derived from LiDAR data were generated and related to the field data. The regression model for maximum heights shows an  $R^2 = 64\%$  for the two observations (Figure 4A). However, a better model fit was generated when relating mean heights between field and TLS. The regression model shows a higher  $R^2 = 88\%$

(Figure 4B). These results may suggest that TLS may not be able to detect point clouds in upper canopies, or those that can be occluded by other under-canopy dense vegetation. This study also shows that the use of terrestrial LiDAR technology can capture accurate understory information.

### Referenced Biomass

Brown (1997) suggested the use of quadratic mean stem diameter (QMSD) as a better choice, as compared to the average DBH, particularly for wide diameter class. The QMSD method is further explained in the Methods section. Table 1 shows an example for a computation of plot biomass in Lake Venado 1 using QMSD

**TABLE 1** Lake Venado 1 plot biomass using quadratic mean stem diameter (QMSD)

| Description   | Diameter at breast height (DBH) class (cm) |          |           |           |           |           |            |
|---|--|----------|-----------|-----------|-----------|-----------|------------|
|   | 5–50                                       | 51–100   | 101–150   | 151–200   | 201–250   | 251–300   | >301       |
| Number of trees present in plot                                   | 21   | 5        | 3         | 3         | 1         | 1         | 1          |
| Quadratic mean stem diameter (i.e., midpoint of class, in cm)     | 22.7                                       | 72.5     | 131.6     | 165.6     | 222.0     | 299.0     | 376.0      |
| Biomass of tree at midpoint (kg tree <sup>-1</sup> ) <sup>a</sup> | 105.69                                     | 2,173.78 | 12,662.96 | 20,051.37 | 33,589.56 | 56,198.81 | 120,209.80 |
| Biomass of all trees (Mg plot <sup>-1</sup> ) <sup>b</sup>        | 2.21                                       | 10.86    | 37.98     | 60.15     | 33.58     | 56.19     | 120.21     |
| Total above-ground biomass (Mg plot <sup>-1</sup> )               | 321.23                                     |          |           |           |           |           |            |

**NOTES**

<sup>a</sup> Using the equation from Chave et al. (2005)

<sup>b</sup> Biomass of all trees = (Number of trees present in plot × Biomass of tree at midpoint) / 1000

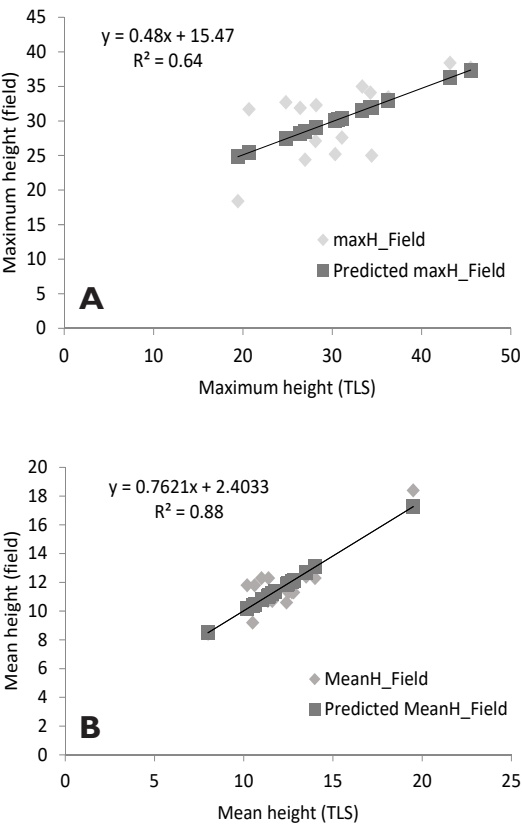


**FIGURE 4** Regression model for maximum height (A) and mean height (B) from field and terrestrial LiDAR system (TLS) data

approach. The referenced plot biomass for the 16 plots are shown in Table 2. Information for each plot also contains range of values for DBH and H, as well as mean biomass computed from three tropical equations. Higher values for mean biomass are shown for plots with high range for DBH values. Biomass values from Chave et al. (2005) provided intermediate values between Brown (1997) and Ketterings et al. (2001). Brown (1997) was based on old forest inventories (i.e., 1970s or earlier) from various countries and used by Food and Agriculture Organization (FAO) of the United Nations to estimate plot to country-level forest biomass (Saket et al. 2005). Brown (1997) is biased to commercial timber. Chave et al. (2005) equation was developed using time series data from 1950 to 2005 from three tropical forests in America, Asia, and Oceania. Meanwhile, Ketterings et al. (2001) established a site-specific allometric equation using destructive sampling in mixed secondary forest in Sumatra, Indonesia.

Biomass values were converted to carbon content by a factor of 0.5 (Westlake 1966). Table 3 displays plot-level carbon stock estimates by management zone and land cover type. The comparison for the mean carbon values consistently showed that SPZ has the highest carbon storage (mean C = 173 Mg C plot<sup>-1</sup>). Plots in the SPZ are open-canopy forest type, while RZ has closed-canopy type. Cultivated areas and mahogany plantations are found in the MUZ. SPZ is characterized by trees with H range of 6 to 441 m and DBH range of 2.6 to 27 cm in the Lake Venado areas. The endemic species, Tinikaran



**TABLE 2** Referenced plot biomass from three allometric equations

| Plot | Location                  | Diameter at breast height (cm) | Height (m) | Mean biomass (Mg plot <sup>-1</sup> ) |                          |                     |
|------|---------------------------|--------------------------------|------------|---------------------------------------|--------------------------|---------------------|
|      |                           |                                |            | Brown (1997)                          | Ketterings et al. (2001) | Chave et al. (2005) |
| 1    | Hotmud                    | 20.0–145.0                     | 2.8–24.4   | 251.7635                              | 88.1334                  | 102.6893            |
| 2    | Antapan                   | 21.0–432.0                     | 2.9–30.2   | 1165.9970                             | 360.1668                 | 347.2175            |
| 3    | Sayaban High School       | 15.0–136.0                     | 3.1–18.4   | 323.2434                              | 112.9900                 | 104.2796            |
| 4    | Sayaban Elementary School | 64.0–138.0                     | 6.6–31.7   | 325.3590                              | 112.8400                 | 112.4940            |
| 5    | Bongolanon                | 11.5–206.0                     | 2.3–27.6   | 247.7589                              | 85.5757                  | 103.7921            |
| 6    | Tawasan 1                 | 13.0–252.0                     | 4.7–32.3   | 459.3474                              | 155.3211                 | 128.2037            |
| 7    | Tawasan 2                 | 27.0–184.0                     | 8.5–32.7   | 293.4051                              | 103.4965                 | 166.5663            |
| 8    | Tawasan 3                 | 15.0–200.0                     | 4.4–31.9   | 283.4871                              | 100.3849                 | 131.4420            |
| 9    | New Israel 1              | 9.5–280.0                      | 2.1–35.0   | 424.2322                              | 160.8764                 | 255.7743            |
| 10   | New Israel 2              | 13.0–196.0                     | 3.0–34.1   | 380.9687                              | 129.7652                 | 200.8526            |
| 11   | New Israel 3              | 15.0–233.0                     | 5.3–33.4   | 305.0471                              | 114.6014                 | 168.2060            |
| 12   | Matiaw 1                  | 14.0–237.0                     | 4.5–37.7   | 435.9379                              | 148.3309                 | 215.9812            |
| 13   | Matiaw 2                  | 13.0–161.0                     | 6.4–25.0   | 206.5257                              | 69.0125                  | 87.1752             |
| 14   | Matiaw 3                  | 10.0–186.0                     | 3.9–38.4   | 289.4739                              | 98.4986                  | 159.7602            |
| 15   | Lake Venado 1             | 10.0–376.0                     | 3.0–27.1   | 971.5203                              | 281.4299                 | 321.2298            |
| 16   | Lake Venado 2             | 6.5–441.0                      | 2.6–25.2   | 1367.4650                             | 368.6408                 | 371.8705            |

**TABLE 3** Plot-level carbon stock estimates by management zone and land cover type

| Management zone   | Land cover type      | N (plots) | Mean carbon (Mg C plot <sup>-1</sup> ) |                          |                     |
|-------------------|----------------------|-----------|--|--------------------------|---------------------|
|                   |                      |           | Brown (1997)                           | Ketterings et al. (2001) | Chave et al. (2005) |
| Multiple use      | Cultivated area      | 9         | 169.0472                               | 59.76951                 | 76.20059            |
| Strict protection | Open-canopy forest   | 2         | 584.7463                               | 162.5177                 | 173.2751            |
| Restoration       | Closed-canopy forest | 5         | 234.9698                               | 76.41422                 | 91.28234            |

(*Leptospermum polygalifolium* Salisb.), are mostly tagged especially in the Lake Venado. There is an ongoing reforestation project in the SPZ and RZ where Tinikaran seedlings are mostly planted. The carbon values differ between the allometries used, where Brown (1997) were two times bigger than Chave et al. (2005).

**Biomass Estimation I**

Three allometric equations were compared using linear and logarithmic models to evaluate how the independent variables relate to AGB (Table 4). The generalized linear model use maximum likelihood estimation (GLM/MLE) to fit the model. It is a nonlinear estimation method. The test statistics of MLE follows a chi-square distribution. For nonlinear models, indices such as minimum Akaike Information Criterion

corrected (AICc), minimum deviance, minimum Pearson value, or maximum likelihood function can be used to compare model validity. In this case, the model with lower AICc was chosen to depict goodness of fit. AICc is defined as AIC with a correction factor for finite sample size or when there is a large number of parameter (k). This study considered a small number of observations, with n = 16 and k = 8. AICc is expressed as follows:

$$AICc = AIC + \frac{2k(k+1)}{n-k-1}$$

(10)

Results of the logarithmic model from using the Brown (1997) allometric equation shows the model is valid at α = 0.05 level. Five independent variables also proved to be significant: mean

**TABLE 4** Summary of regression results using percentile heights

| Equation                | Stepwise regression |        | Generalized linear model (GLM) |                     | Model selected     |
|-------------------------|---------------------|--------|--------------------------------|---------------------|--------------------|
|                         | R <sup>2</sup>      | F-stat | AICc                           | Prob>X <sup>2</sup> |                    |
| Brown (1997)            |                     |        |                                |                     |                    |
| Linear model            | 0.49                | 0.5937 | 240.00                         | 0.3080              | GLM with lower AIC |
| Log-log model           | -                   |        | 73.70                          | 0.0351 <sup>a</sup> |                    |
| Chave et al. (2005)     |                     |        |                                |                     |                    |
| Linear model            | 0.50                | 0.5622 | 241.97                         | 0.1890              | GLM with lower AIC |
| Log-log model           | -                   |        | 68.87                          | 0.0560 <sup>b</sup> |                    |
| Kettering et al. (2001) |                     |        |                                |                     |                    |
| Linear model            | 0.45                | 0.6706 | 244.00                         | 0.2897              | GLM with lower AIC |
| Log-log model           | -                   |        | 71.31                          | 0.0608 <sup>b</sup> |                    |

**NOTES:** <sup>a</sup> Model is significant at  $\alpha = 0.05$  <sup>b</sup> Model is significant at  $\alpha = 0.10$

height, as well as percentile heights at the 25th, 50th, 75th, and 95th levels. The final equation for the predictive model is written as follows:

$$AGB = \frac{\exp(3.56) \times \text{meanH}^{68.9} \times \text{Per25H}^{-11.08} \times \text{Per50H}^{-17.09} \times \text{Per75H}^{-15.71} \times \text{Per95H}^{-11.18}}{\text{Per50H}^{-17.09} \times \text{Per75H}^{-15.71} \times \text{Per95H}^{-11.18}} \quad (11)$$

Based on Chave et al. (2005) allometric equation, the MLE model is significant at  $\alpha = 0.10$ . There were two regressors that were significant at  $\alpha = 0.05$  level. These are percentile heights at the 50th and 95th levels. Equation 3 shows the final equation for the predictive model.

$$AGB = \exp(5.51) \times \text{Per50H}^{-12.0} \times \text{Per95H}^{-9.98} \quad (12)$$

The final equation from Ketterings et al. (2001) showed that the logarithmic model is significant at  $\alpha = 0.10$  level. There are also five independent variables that are significant at  $\alpha = 0.05$  level. These are mean height and percentile heights at the 25th, 50th, 75th, and 95th levels. The final equation is written as follows:

$$AGB = \frac{\exp(3.27) \times \text{meanH}^{58.13} \times \text{Per25H}^{-9.16} \times \text{Per50H}^{-14.95} \times \text{Per75H}^{-13.13} \times \text{Per95H}^{-9.79}}{\text{Per50H}^{-14.95} \times \text{Per75H}^{-13.13} \times \text{Per95H}^{-9.79}} \quad (13)$$

## Biomass Estimation II

The second biomass estimation approach displays the statistical relationship between normalized height bins to AGB. Unlike the GLM/MLE model, standard least square is a

linear model which uses stepwise regression to fit the model. The test statistic is an F-test, where information for regression sum of square (SSR) and total sum of square (SST) are given, enabling the computation of R<sup>2</sup>. The index R<sup>2</sup> explains the linear relationship between dependent and independent variables. A variance inflation (VIF) index detects the presence of multicollinearity in the data. A VIF index larger than 10 denotes presence of multicollinearity.

Stepwise regression showed a better model performance for relating height bins in predicting AGB level (Table 5). The R<sup>2</sup> level for each model are at mid-50% level, which may suggest that there are other unexplained factors that were not captured with these given independent variables.

Results from an analysis of variance (ANOVA) for the Brown (1997) allometric equation showed that the model is valid at  $\alpha = 0.05$  level. The significant predictors are NHBin25 and NHBin 30. Both independent variables have VIF = 2.18, implying an absence of any multicollinearity issues. The final equation is written as follows:

$$AGB = 4396.79 \times 2651839.9 \text{ NHbin25} \times -6336060 \text{ NHBin30} \quad (14)$$

ANOVA results from the Chave et al. (2005) allometric equation showed that the model is valid at  $\alpha = 0.05$  level. The only significant predictor is NHBin25 with VIF = 2.21. The final equation is written as follows:

**TABLE 5** Summary of regression results using normalized height bins

| Equation                | Stepwise regression |                     | Generalized linear model (GLM) |                     | Model selected      |
|-------------------------|---------------------|---------------------|--------------------------------|---------------------|---------------------|
|                         | R <sup>2</sup>      | F-stat              | AICc                           | Prob>X <sup>2</sup> |                     |
| Brown (1997)            |                     |                     |                                |                     |                     |
| Linear model            | 0.52                | 0.0080 <sup>a</sup> | 299.88                         | 0.0159 <sup>a</sup> | Stepwise regression |
| Log-log model           | -                   |                     | -                              |                     |                     |
| Chave et al. (2005)     |                     |                     |                                |                     |                     |
| Linear model            | 0.46                | 0.0175 <sup>a</sup> | 259.06                         | 0.0335 <sup>a</sup> | Stepwise regression |
| Log-log model           | -                   |                     | -                              |                     |                     |
| Kettering et al. (2001) |                     |                     |                                |                     |                     |
| Linear model            | 0.44                | 0.0226 <sup>a</sup> | 260.87                         | 0.0457 <sup>a</sup> | Stepwise regression |
| Log-log model           | -                   |                     | -                              |                     |                     |

**NOTES:** <sup>a</sup> Model is significant at  $\alpha = 0.05$

$$AGB = \frac{2608.39 \times 613949.8 \text{ NHbin25} \times -948818.8 \text{ NHBin30}}{(15)}$$

The ANOVA results from the Ketterings et al. (2001) equation also showed that the model is valid at  $\alpha = 0.05$  level. Like the Brown (1997) equation, NHBin25 and NHBin30 are significant predictors with VIF = 2.18, implying absence of data multicollinearity issues. The final equation is written as follows:

$$AGB = \frac{593.9 \times 652758.41 \text{ NHbin25} \times -1542118 \text{ NHBin30}}{(16)}$$

The predictive models generated provided an insight on how percentile heights and normalized height bins relate to estimating plot-level AGB. It may be easier for the user to identify height bins at 5-m interval than using percentile heights. The use of wood density information from allometries developed by Chave et al. (2005) and Ketterings et al. (2001) would provide additional variability in addition to height and DBH information.

The regression models relating reference AGB to TLS height metrics had identified significant variables useful for biomass estimation. Variables selection techniques like GLM/MLE and stepwise regression also were useful in presenting how TLS height variables predict AGB. The various algorithms presented will be helpful in assessing carbon at plot-level using non-destructive sampling approach.

Summary and Conclusion

Tropical forests are among the most carbon-rich ecosystems in the world, with the ability to sequester carbon through reforestation, agroforestry, and conservation of existing forests. Mt. Apo Natural Park contains hardwood tree species that have massive diameters of  $\geq 300$  cm.

A referenced biomass was used to relate to the TLS-derived metrics. These referenced biomasses were computed using the three tropical allometric equations from Brown (1997), Ketterings et al. (2001), and Chave et al. (2005). Destructive sampling was not permitted inside the MANP protected area. To compute plot biomass with large DBH intervals, Brown (1997) suggested using quadratic mean stem diameter for each DBH class to be used as a midpoint tree.

The allometric equations considered in this study reported a good modeling fit with the DBH classes. The predictive models generated provided an insight on how percentile heights and normalized height bins relate to estimating plot-level AGB. It was recommended to identify height bins at 5-m interval than using percentile heights. Stepwise regression showed a good model fit in relating height bins to referenced biomass. The use of wood density information from allometries developed by Chave et al. (2005) and Ketterings et al. (2001) provided additional biomass information, in addition to height and DBH information. This study also demonstrated how the estimated carbon stocks differ between three allometric equations. Brown (1997)

consistently showed the highest values, while Chave et al (2005) provided the intermediate values. Ketterings et al. (2001) was developed using site-specific estimates, and Brown (1997) is biased to commercial timber.

Our research has demonstrated the adoption of IPCC's Tier 2, a combination of field and remote sensing data, in the assessment of available biomass levels in a tropical forest.

Far-flung areas limit the accessibility for doing field inventory inside this park. Local insurgency restricted our access to the northern portion of the park. The use of terrestrial LiDAR technology captured accurate understory information, which is helpful in extraction of tree metrics. The algorithms developed are beneficial for future research work to extrapolate the biomass levels to landscape and park level using available multispectral or radar imagery.

Our study demonstrated the biomass modeling study that needs to be conducted in this national park. In compliance to REDD requirements, our study also characterized carbon content by management zone and forest types. These results will provide important insights to various stakeholders, both government and civic organizations, who are keepers of this cultural heritage for effective land-use management. The results generated showed the ecological importance of these hardwood species and their significance in storing carbon stocks. These findings will be used to generate a baseline carbon stocks information for MANP, which is considered as an important forest ecosystem in the country.

## Acknowledgment

We are grateful to the Department of Environment and Natural Resources (Regions XI and XII), which provided the research permit, and to the Philippine National Police of Region XII for providing the security escorts. We are also grateful to the Mt. Apo Foundation, Inc. for granting us the written permission to use and for referencing their land cover maps. Thanks also to our research assistants for the invaluable support during our rigorous fieldwork activities.

## References

- BROWN S. 1997. Estimating biomass and biomass change of tropical forests: a primer. FAO Forestry Paper no. 134. Rome: FAO.
- CHAVE J, ANDALO C, BROWN S, CAIRNS MA, CHAMBERS JQ, EAMUS D, FOLSTER H, FROMARD F, HIGUCHI N, KIRA T, LESCURE JP, NELSON BW, OGAWA H, PUIG H, RIERA B, YAMAKURA T. 2005. Tree allometry and improved estimation of carbon stocks and balance in tropical forests. *Oecologia* 145: 87–99. DOI 10.1007/s00442-005-0100-x.
- DRAKE JB, DUBAYAH RO, CLARK DB, KNOX RG, BLAIR JB, HOFTON MA, CHAZDON RL, WEISHAMPEL JE, PRINCE SD. 2002. Estimation of tropical forest structural characteristics using large-footprint LiDAR. *Remote Sens. Environ.* 79: 305–319.
- HAN SR, WOO SY, LEE DK. 2010. Carbon storage and flux in aboveground vegetation and soil of sixty-year-old secondary natural forest and large leafed mahogany (*Swietenia macrophylla* King) plantation in Mt. Makiling, Philippines. *Asia Life Sci.* 19(2): 357–372.
- KETTERINGS QM, COE R, VAN NOORDWIJK M, AMBAGAU Y, PALM CA. 2001. Reducing uncertainty in the use of allometric biomass equations for predicting above-ground tree biomass in mixed secondary forests. *Forest Ecol. Manag.* 146: 199–209.
- LASCO RD, GUILLERMO IQ, CRUZ RV, BANTAYAN NC, FB PULHIN. 2004. Carbon stocks assessment of a secondary forest in Mount Makiling Forest Reserve, Philippines. *J. Trop. For. Sci.* 16: 35–45.
- LASCO RD, MACDICKEN KG, PULHIN FB, GUILLERMO IQ, SALES RF, CRUZ RV. 2006. Carbon stocks assessment of a selectively logged Dipterocarpaceae forest and wood processing mill in the Philippines. *J. Trop. For. Sci.* 18: 212–221.
- LEFSKY MA. 2010. A global forest canopy height map from the moderate resolution imaging spectroradiometer and the Geoscience Laser Altimeter System. *Geophys. Res. Lett.* 37: L15401.
- LEWIS RE. 1988. Mt. Apo and other national parks in the Philippines. *Oryx* 22(2): 100–109.
- OLANDER LP, GIBBS HK, STEININGER M, SWENSON JJ, MURRAY BC. 2008. Reference scenarios for deforestation and forest degradation in support of

- REDD: a review of data and methods. *Environ. Res. Lett.* 3. doi:10.1088/1748-9326/3/2/025011.
- PUESCHEL P. 2013. The influence of scanner parameter on the extraction of tree metrics from FARO Photon 120 terrestrial laser scans. *ISPRS J. Photogramm. Remote Sens.* 78: 58–68.
- RIBEIRO, N.S., MATOS, C., MOURA, I., WASHINGTON-ALLEN, R.A., AND RIBEIRO, A. 2013. Monitoring vegetation dynamics and carbon stock density in miombo woodlands. *Carbon Balance Manag.* 8:11
- SAKET M, ALTRELL D, BRNATHOMME A, VUORINEN P. 2005. *FAO's approach to support national forest assessments for country capacity building*. Rome: FAO.
- WESTLAKE DF. 1966. The biomass and productivity of *Glyceria maxima*: I. Seasonal changes in biomass. *J. Ecol.* 54: 745–753.